

Numerical and experimental investigations of 14 different small wind turbine airfoils for 3 different Reynolds number conditions

Cevahir Tarhan* and Ilker Yilmaz^a

Erciyes University, Faculty of Aeronautics and Astronautics, Kayseri, 38280, Turkey

(Received March 9, 2018, Revised September 20, 2018, Accepted September 25, 2018)

Abstract. In this study, we have focused on commonly used 14 different small wind turbine airfoils (A18, BW3, Clark Y, E387, FX77, NACA 2414, RG 15, S822, S823, S6062, S7012, SD6060, SD7032, SD7062). The main purpose of the study is to determine the lift, drag and lift/drag coefficients of these airfoils with numerical analysis and to verify 2 best airfoil's results with experimental analysis. Airfoils were determined from past studies on small wind turbines. Numerical analyzes of the airfoils were done with Ansys Fluent fluid dynamics program. Experimental analyzes were done at wind tunnel in Erciyes University, Turkey. Lift and drag coefficients of these airfoils were determined for 50,000-100,000-200,000 Reynolds numbers.

Keywords: wind turbine; airfoil; lift, drag

1. Introduction

Mostly wind energy has been producing from large wind turbines but small wind turbines also have a great potential for energy production. In this study we performed wind flow simulations for 14 types of (A18, BW3, Clark Y, E387, FX77, NACA 2414, RG 15, S822, S823, S6062, S7012, SD6060, SD7032, SD7062) small scale wind turbine airfoils which are commonly used in small wind turbines (Vardar and Alibas 2008). These airfoils were compiled from past studies. Karthikeyan *et al.* (2015) have studied 15 different airfoils for the Reynolds numbers below 500,000 which are used in wind turbines. Most of these airfoils were considered in this study. Tangler and Somers (1995) investigated the use of NACA type and S type airfoils in wind turbines. These airfoils were also taken into account in this study. Fuglsang and Madsen (1999) tried to optimize wind turbine rotors with numerical optimization. Henriques *et al.* (2009) designed a new urban wind turbine airfoil using pressure load inverse method. Sadikin *et al.* (2018) studied to determine NACA0012 airfoil's characteristics. After the simulation of the 2D steady NACA0012 airfoil, found realizable k-epsilon turbulence model as best turbulence model for 2D steady analysis. Daroczy *et al.* (2015) also researched and compared turbulence models for wind turbine CFD analysis and found k-epsilon realizable as best turbulence model for analysis. Giguere and Selig (1997) studied some low Reynolds Number airfoils for small horizontal axis wind turbines and they have found their characteristics. Buhagiar and Sant (2014) researched steady state analysis of a conceptual offshore wind turbine.

Khamlaj and Rumpfkeil (2018) performed analysis and optimization of ducted wind turbines with a steady computational model.

The main purpose of the study is to determine the lift, drag and lift/drag coefficients of these 14 airfoils with numerical analysis and to verify 2 best airfoils results with experimental analysis. Simulations and experiments were performed for 50,000-100,000-200,000 Reynolds numbers. Ansys Fluent fluid dynamics program was used for simulations. Experimental analyzes were done at wind tunnel in Erciyes University, Turkey. $(C_l/C_d)_{max}$ and C_{lmax} parameters were chosen for evaluation process. This is because of the dependency of efficiency to high lift coefficient and low drag coefficient while converting wind power to torque power.

2. Numerical scheme

In analyzes; the pressure based solution method, which gives more accurate results for the incompressible flows; was used for Ansys Fluent fluid dynamics program analyzes. Also the k-epsilon realizable turbulence model and standard wall function was preferred in the analyzes, because of the similarity of the results to experimental study and past studies on 2D steady airfoils analysis. In order to avoid calculation errors, double precision was set. Second order discretization was chosen for pressure, momentum and other parameters. Analyses were continued up to 1×10^{-6} residuals left. $20c \times 20c$ 2D flow area was meshed with 110749 nodes and used for analyzes. For ensuring grid independency, flow area was meshed with 4 different number of node cells. Higher number of node cells didn't change the results after 110749 node cells. So average of 110749 node cells was used for the meshes. Mesh density around the airfoils was increased for accurate analysis of the flow. Meshed flow area around the A18 airfoil is given

*Corresponding author, Lecturer
E-mail: ctarhan@erciyes.edu.tr

^a Professor
E-mail: ctarhan@erciyes.edu.tr

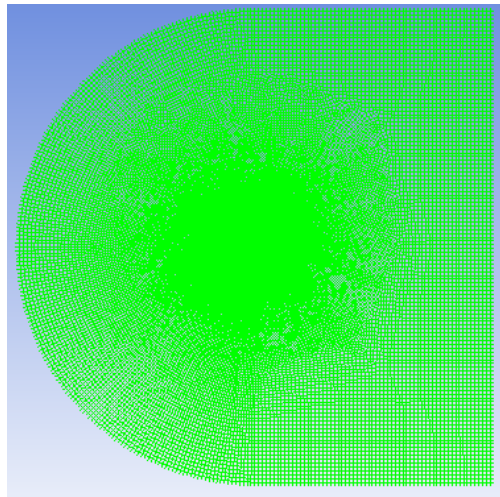


Fig. 1 Meshed flow area around the A18 airfoil

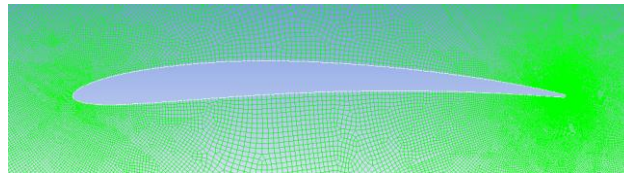
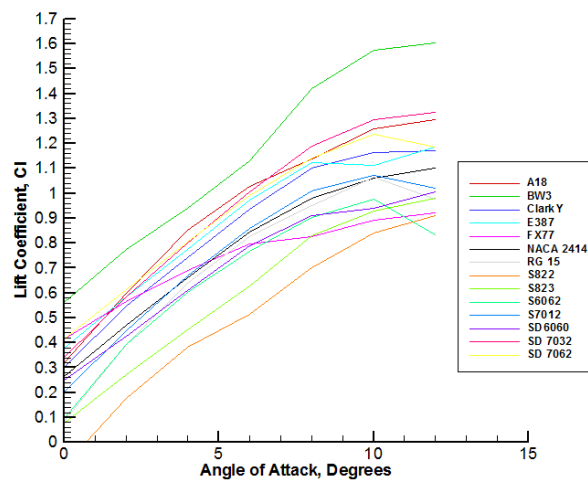


Fig. 2 Close view of mesh structure around the A18 airfoil

Fig. 3 Lift coefficient curves for the airfoils at $Re=50,000$

in Figs. 1 and 2. Calculations were done for uniform steady wind speeds.

C_l/C_d max ratio was determined as first evaluation criterion for determining best suiting airfoil for wind turbine usage. For obtaining (C_l/C_d) max ratio, first of all C_l and C_d coefficients values were determined for chosen airfoils after the performed simulations with Ansys Fluent fluid dynamics program for 50,000-100,000-200,000 Reynolds numbers. C_l , C_d and C_l/C_d coefficient values of the airfoils for 50,000 Reynolds number were given in Figs. 3-5.

As seen in Fig. 3; BW3 airfoil has the highest lift coefficient value and the second best lift coefficient value is for A18 airfoil for angle of attacks from 0° to 12° . For S6062, RG15, SD7062 and S7012 airfoils; stall was occurred at 10° angle of attack. Fig. 2 shows us the drag coefficients of the airfoils and that BW3 airfoil has far better drag coefficient value for angle of attacks from 0° to 12° when compared with other airfoils, as seen in Fig. 4. Low drag coefficient results of BW3 gives us the best airfoil C_l/C_d ratio value among all airfoils as seen in Fig. 5.

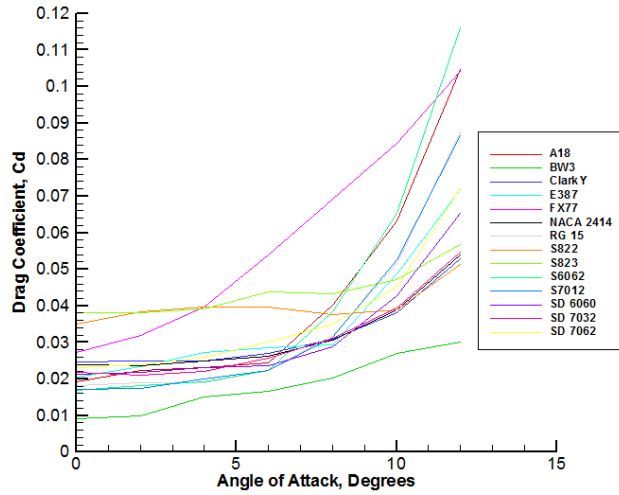


Fig. 4 Drag coefficient curves for the airfoils at $Re=50,000$

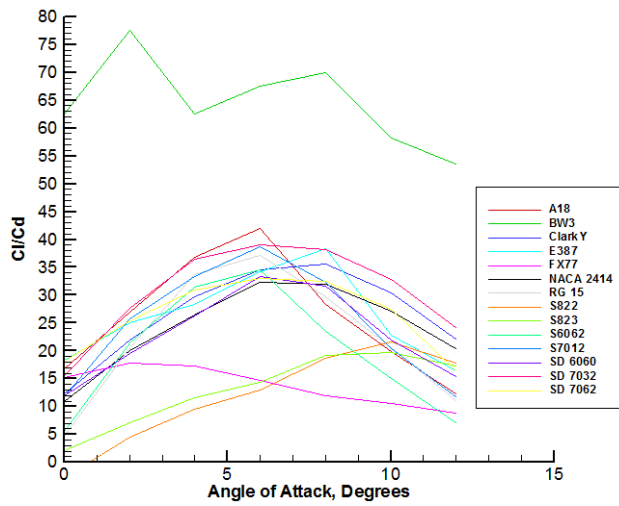


Fig. 5 Lift coefficient / drag coefficient curves for the airfoils at $Re= 50,000$

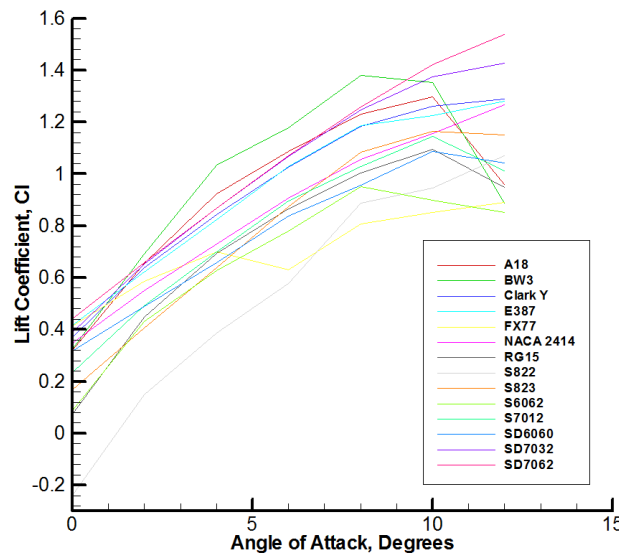


Fig. 6 Lift coefficient curves for the airfoils at $Re=100,000$

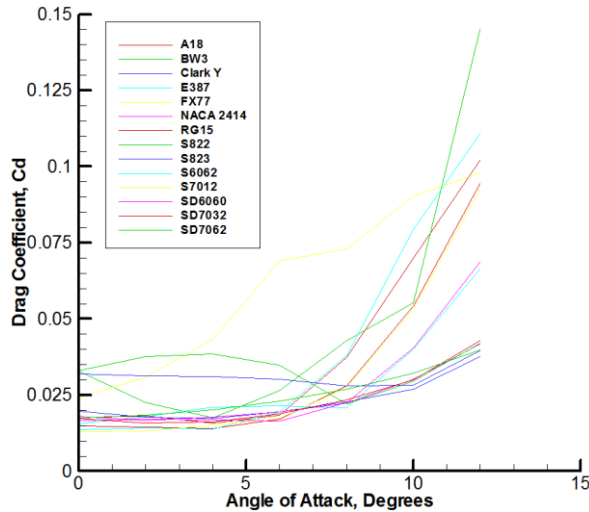


Fig. 7 Drag coefficient curves for the airfoils at Re=100,000

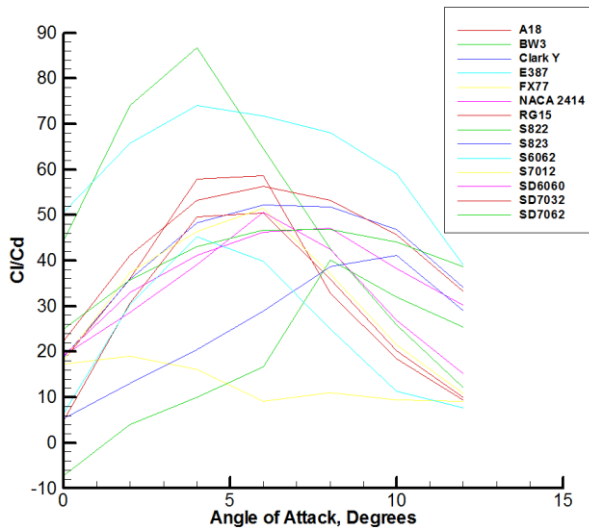


Fig. 8 Lift coefficient / drag coefficient curves for the airfoils at Re= 100,000

C_l, C_d and C_l/C_d coefficient values of the airfoils for 100,000 Reynolds number were given in Figs. 6-8.

As seen in Fig. 3; BW3 airfoil has the highest lift coefficient value and the second best lift coefficient value is for A18 airfoil for angle of attacks from 0^0 to 12^0 . For S6062, RG15, SD7062 and S7012 airfoils; stall was occurred at 10^0 angle of attack. Fig. 2 shows us the drag coefficients of the airfoils and that BW3 airfoil has far better drag coefficient value for angle of attacks from 0^0 to 12^0 when compared with other airfoils, as seen in Fig. 4. Low drag coefficient results of BW3 gives us the best airfoil C_l/C_d ratio value among all airfoils as seen in Fig. 5.

C_l, C_d and C_l/C_d coefficient values of the airfoils for 100,000 Reynolds number were given in Figs. 6-8.

In Fig. 6 BW3 airfoil has the highest lift coefficient value for 0^0 - 12^0 angle of attacks. For S823, RG15 and E387 airfoils; stall was occurred at 10^0 angle of attack. For BW3 and S7012 airfoils; stall was occurred at 8^0 angle of attack.

Fig. 7 shows us the drag coefficient values of the airfoils and most of the airfoils have similar low drag coefficient values for angle of attacks between 0^0 to 12^0 . Better lift coefficient values of BW3 airfoil gives us the best airfoil C_l/C_d ratio among all airfoils as seen in Fig. 8.

C_l, C_d and C_l/C_d coefficient values of the airfoils for 200,000 Reynolds number were given in Fig. 9-11.

As seen in Fig. 9 BW3 and A18 airfoils have the highest lift coefficient values between 0^0 - 12^0 angle of attacks. For BW3, FX77, S7012 and A18 airfoils; stall has been occurred at 10^0 angle of attack. For S6062 airfoil, stall was occurred at 8^0 angle of attack. Fig. 10 shows us the drag coefficient values of the airfoils and most of the airfoils have similar low drag coefficient values for angle of attacks between 0^0 - 12^0 . Higher lift coefficient values of the A18 airfoil makes this airfoil best for 200,000 Reynolds number among all airfoils as seen in Fig. 11.

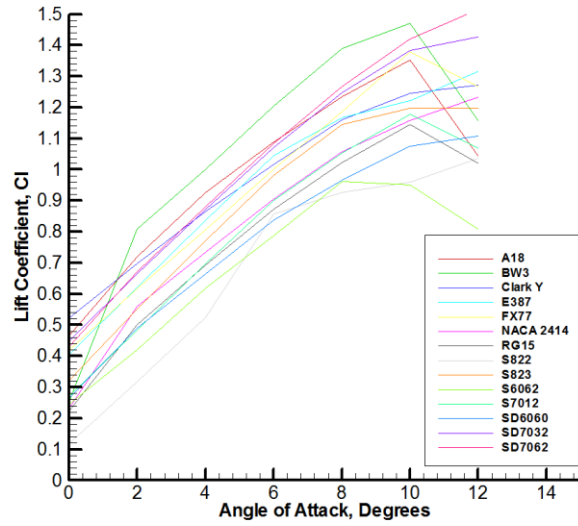


Fig. 9 Lift coefficient curves for the airfoils at Re=200,000

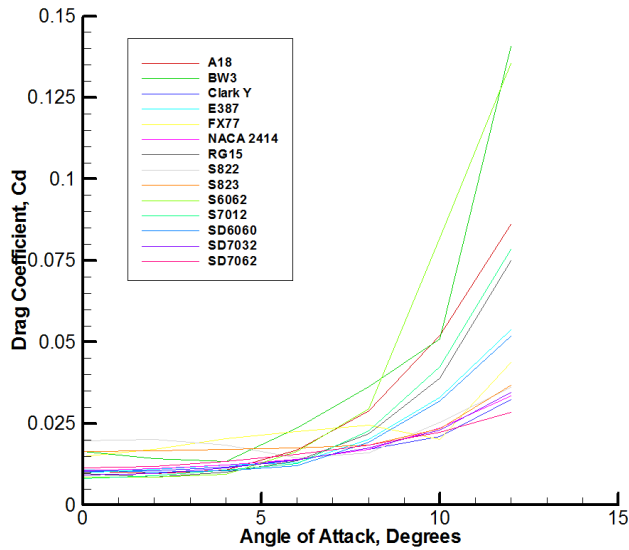


Fig. 10 Drag coefficient curves for the airfoils at Re=200,000

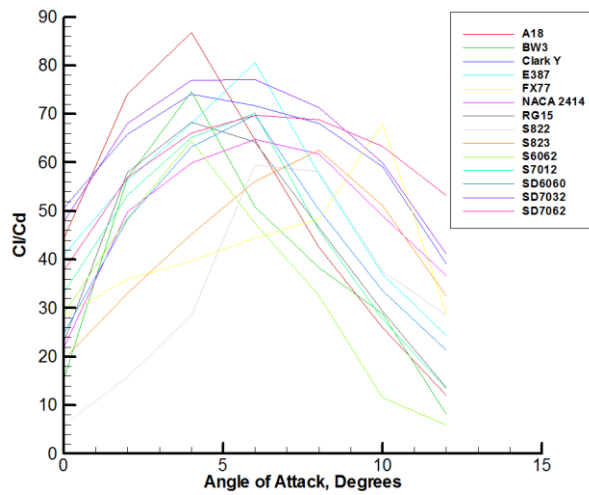


Fig. 11 Lift coefficient / drag coefficient curves for the airfoils at Re= 200,000

Table 1 Performance parameters for the airfoils considered

Airfoil	$(C_l/C_d)_{\max}$ for 50,000 Reynolds Number	$(C_l/C_d)_{\max}$ for 100,000 Reynolds Number	$(C_l/C_d)_{\max}$ for 200,000 Reynolds Number
A18	42.50	58,61	86,73
BW3	77.00	86,73	74,66
Clark Y	35.48	52,28	74,04
E387	38.62	74,04	80,65
FX77	18.06	18,99	68,05
NACA2414	32.30	47,0	64,75
RG15	37.27	50,44	68,36
S822	21.53	40,13	59,51
S823	19.78	41,1	62,48
S6062	35.00	45,20	64,56
S7012	37.39	51,55	70,10
SD6060	33.33	50,62	63,24
SD7032	38.46	56,26	77,06
SD7062	33.00	46,83	69,78

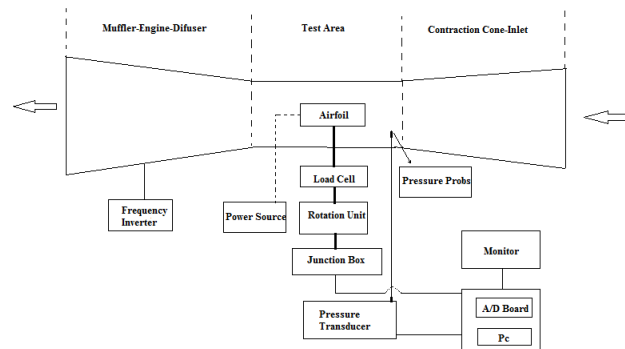


Fig. 12 Schematic diagram of the experimental set-up



Fig. 13 A view of the wind tunnel and the test area

In Table 1, all of the 14 airfoil's evaluated performance parameters were given. $(C_l/C_d)_{\max}$ corresponds to the best value for angle of attacks between 0° - 12° for the airfoils. BW3 airfoil has the highest $(C_l/C_d)_{\max}$ ratio for 50,000 and 100,000 Reynolds Numbers. A18 airfoil has the highest $(C_l/C_d)_{\max}$ ratio for 200,000 Reynolds Number.

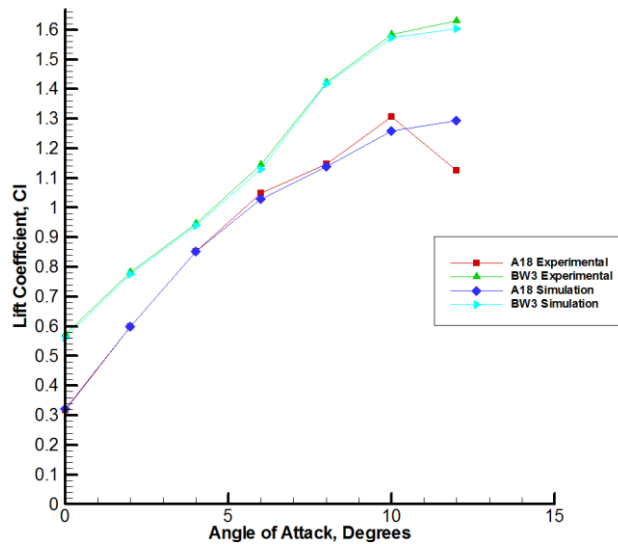
3. Experimental analysis

According to simulation results, A18 and BW3 airfoils

were selected for experimental investigations in the ind tunnel. These airfoils were produced with a 3D printer and analyzed in the wind tunnel for 50,000-100,000-200,000 Reynolds numbers. The experimental setup and schematic diagram of the wind tunnel were given in Fig. 12. A photo of the wind tunnel and the produced A18 airfoil were given on Fig. 13 and Fig. 14. In analysis Ati f/t gamma SI 32-2.5 force/torque sensor was used to determine the forces on the airfoil. Drehachse ZD30 traverse unit was used as rotation unit which is seen behind the airfoil in Fig. 12. Force/torque sensor can measure 3 forces and 3 moments up to 1200N



Fig. 14 A18 airfoil in the test area of wind tunnel


 Fig. 15 Lift coefficient curves for the airfoils at $Re=50,000$

for F_{xy} , 4100N for F_{xz} , 79Nm for T_{xy} and 82 NM for T_z . The manufactured airfoils have a span length of 250 mm, and a chord length of 130 mm. Test area of the wind tunnel is 500 mm*500 mm. The free stream turbulence intensity of the wind tunnel is lower than 0.1% at lowest speed.

The uncertainty of the measurement dependencies are because of the uncertainties of the repeatability, the accuracy of force meter, position of the airfoil, air density, ambient pressure, etc.. The uncertainty values in the, lift force coefficient (U_{Cl}), drag force coefficient (U_{Cd}) and Reynolds number (U_{Re}) were given in Table 2.

The blockage corrections weren't done on the experimental results; because of the blockage effects on the experimental results are negligible when the blockage ratio is less than 10%.

In Fig. 15 experimental and numerical lift coefficient results for 50,000 Reynolds Number were given for the best airfoils (A18 and BW3) which were determined in numerical study. It can be seen that numerical and experimental results have good agreement with each other.

Only a 10 percent of difference exists between the experimental and numerical results of A18 airfoil. And it was considered that this difference is because of the flow separation which occurred at 12° . Surface roughness can change flow separation angle for 1 or 2 degrees for airfoils and this situation affects the data at 12° . In Fig. 16 experimental and numerical drag coefficient results were given for the best two airfoils. Numerical and experimental results have good agreement with each other. In Fig. 17 experimental and numerical lift coefficient / drag coefficient results were given for the airfoils. There is a 5 percent difference for BW3 airfoil between the data of experimental and numerical analysis. This was considered as the result of small measurement errors for the lift and drag coefficients. The data for A18 airfoil is similar for both experimental and numerical analysis. BW3 airfoil has the highest Cl / Cd value at 2° degree angle of attack and A18 airfoil has the highest Cl / Cd value at 6° degree angle of attack which is important for the installation of airfoil to wind turbine.

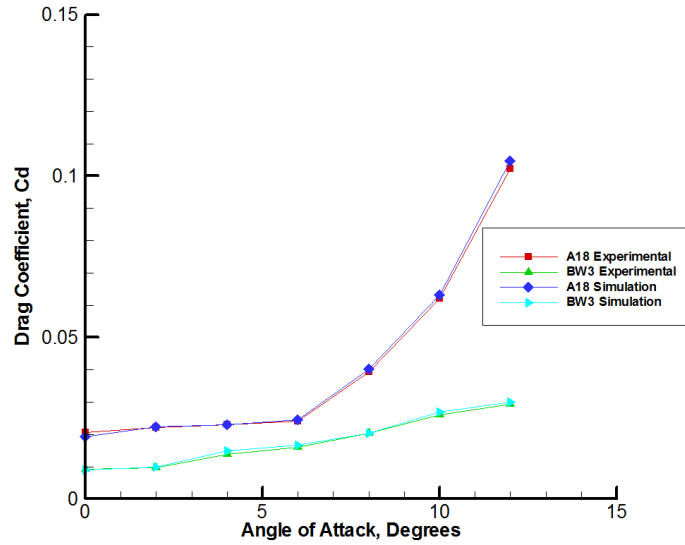


Fig. 16 Drag coefficient curves for the airfoils at Re=50,000

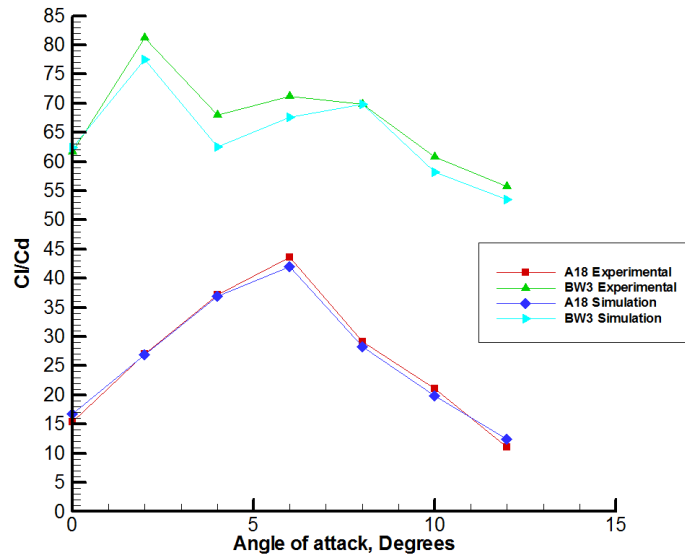


Fig. 17 Lift coefficient / drag coefficient curves for the airfoils at Re= 50,000

Table 2 Uncertainties as % for lift force coefficient (U_{C_L}), drag force coefficient (U_{C_d}) and Reynolds number (U_{Re})

Airfoil	U_{C_L}	U_{C_d}	U_{Re}
50,000	5.1	5.2	5.3
100,000	4.8	4.7	4.6
200,000	4.5	4.3	3.9

In Fig. 18 experimental and numerical lift coefficient results for 100,000 Reynolds Number were given for the best airfoils (A18 and BW3). It can be seen that numerical and experimental results have good agreement with each other. In Fig. 19 experimental and numerical drag coefficient results were given for the best two airfoils. Numerical and experimental results have good agreement

with each other. In Fig. 20 experimental and numerical lift coefficient / drag coefficient results were given for the best two airfoils. There is a 4 percent difference for A18 airfoil between the data of experimental and numerical analyzes. This is considered as the result of small measurement errors for the lift and drag coefficients. The data for A18 airfoil is similar for both experimental and numerical analysis. BW3 airfoil has the highest Cl / Cd value at 40 degree angle of attack and A18 airfoil has the highest Cl / Cd value at 60 degree angle of attack. On Fig. 21 drag polars of the airfoils have been compared with the study of Giguere and Selig (1997). As seen in the figure both studies have good agreement with each other and there is only a 1-2 percent differences between these studies.

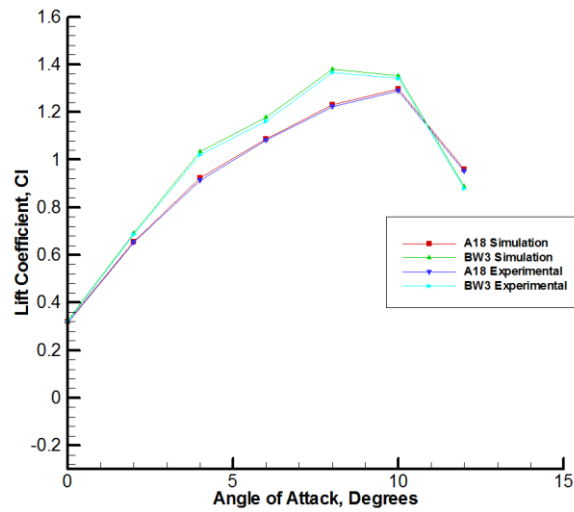


Fig. 18 Lift coefficient curves for the airfoils at Re=100,000

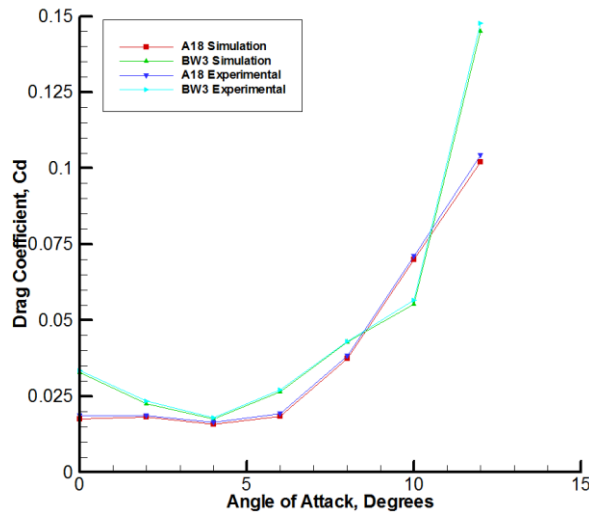


Fig. 19 Drag coefficient curves for the airfoils at Re=100,000

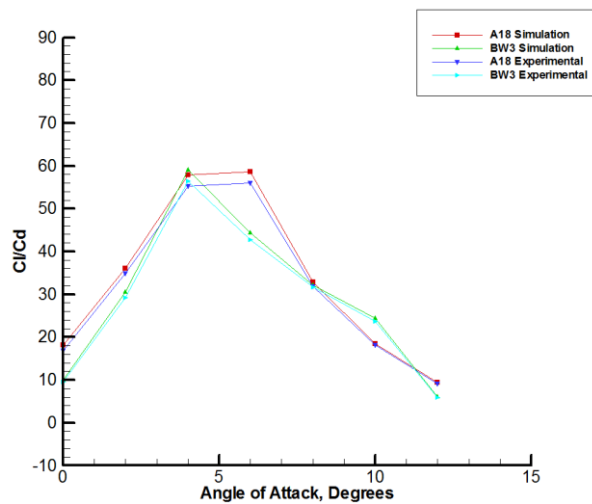


Fig. 20 Lift coefficient / drag coefficient curves for the airfoils at Re= 100,000

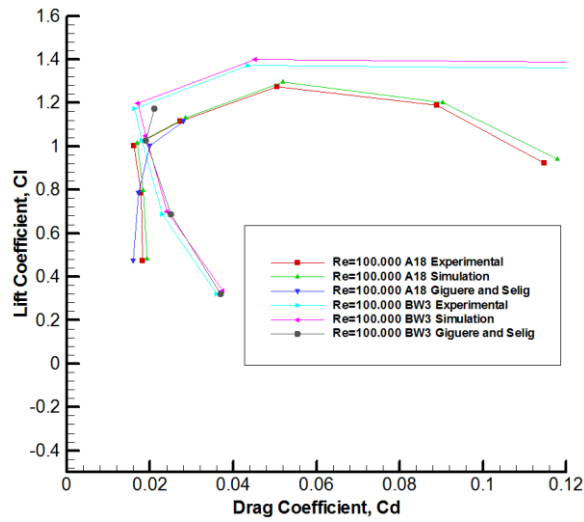


Fig. 21 Drag polars of airfoils for $Re=100,000$ (Giguere and Selig 1997)

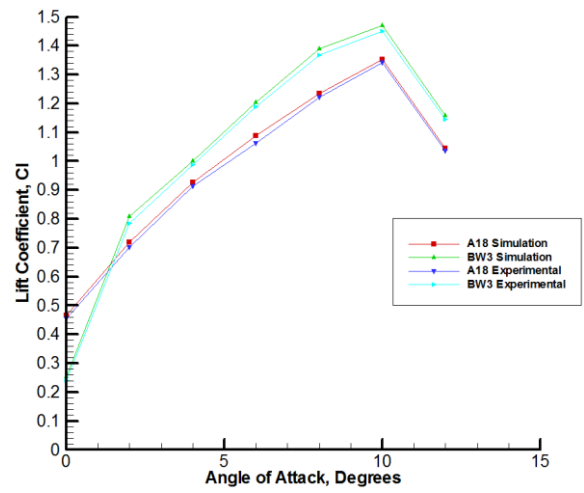


Fig. 22 Lift coefficient curves for the airfoils at $Re=200,000$

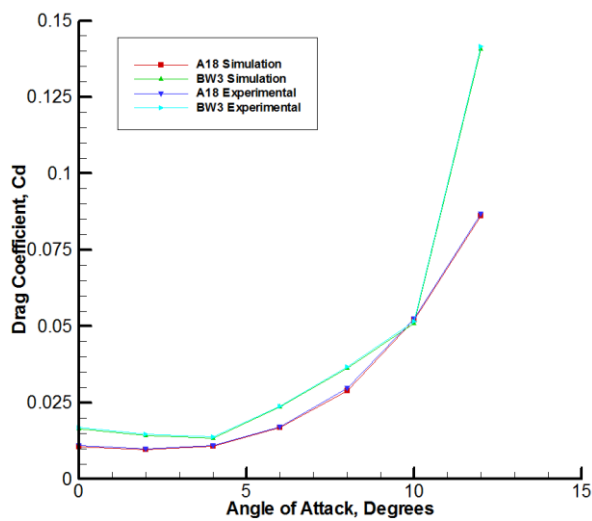


Fig. 23 Drag coefficient curves for the airfoils at $Re=200,000$

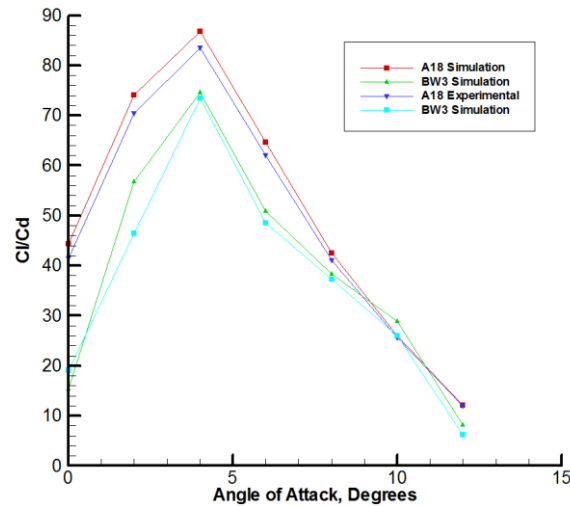


Fig. 24 Lift coefficient / drag coefficient curves for the airfoils at Re= 200,000

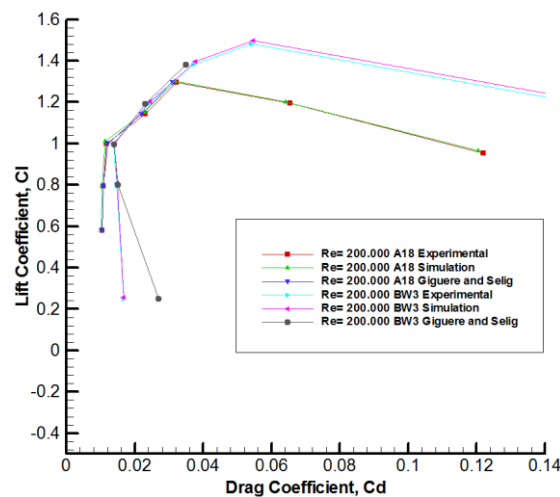


Fig. 25 Drag Polars of Airfoils for Re=200,000 (Giguere and Selig 1997)

In Fig. 22 experimental and numerical lift coefficient results for 50,000 Reynolds Number was given for the best airfoils (A18 and BW3) which were determined from the numerical study. It can be seen that numerical and experimental results have good agreement with each other. Only a 10 percent difference exists between the experimental and numerical results of A18 airfoil. And it was considered that this difference is because of the flow separation which occurred at 12°. Surface roughness may change flow separation angle for 1 to 2 degrees for airfoils and this situation affects the data at 12°. In Fig. 23 experimental and numerical drag coefficient results were given for the best two airfoils. Numerical and experimental results have good agreement. In Fig. 24 experimental and numerical lift coefficient / drag coefficient results were given for the best two airfoils. There is a 5 percent difference for BW3 airfoil between the data of experimental and numerical analysis. This was considered as the result of small measurement errors for the lift and drag coefficients.

The data for A18 airfoil is similar for both experimental and numerical analysis. BW3 and A18 airfoils both have the highest Cl / Cd value at 40 degree angle of attack. In Fig. 25 drag polars of the airfoils were compared with the study of Giguere and Selig (1997). As seen on the figure both studies are similar and there is only a 1-2 percent differences between these studies for the most of the points taken into consideration.

4. Conclusions

BW3 airfoil was evaluated as the best suited airfoil for small wind turbines where the Reynolds Number is 50,000 or 100,000. BW3 has far better Cl/Cd ratio, high lift coefficient value and low drag coefficient value when compared to other chosen small wind turbine airfoils.

Because of the low thickness of A18 and BW3 airfoils when compared with other chosen airfoils; they produce lower drag than most of the investigated airfoils.

For 200,000 Reynolds number most of the airfoils have similar values but A18 airfoil has the highest(Cl/Cd)max ratio. As a result A18 airfoil was considered as best suited airfoil for this Reynolds Number area.

FR

When the lift coefficient data was evaluated alone, it was seen that BW3 airfoil has the highest value of the lift coefficient among the airfoils examined for all Reynolds numbers. This is because of the higher camber line of the BW3 airfoil. Curvature under the BW3 airfoil compresses the flowing air under the profile and this situation increases the lift coefficient of the BW3 airfoil.

During the usage of BW3 airfoil in a wind turbine; it was estimated that the installation with the 2⁰ degree angle of attack, where the profile has the highest Cl / Cd value, will provide the ideal yield for the wind turbines where the Reynolds Number is 50,000 or 100,000.

During the usage of A18 airfoil in a wind turbine; it was estimated that the installation with the 4⁰ degree angle of attack, where the profile has the highest Cl / Cd value, will provide the ideal yield for the wind turbines where the Reynolds Number is 200,000.

Acknowledgements

This study was supported and funded by Erciyes University, Department of Scientific Research Projects, Turkey with a Project ID of FDK-2016-6806.

References

- Buhagiar, D. and Sant, T. (2014), "Steady-state analysis of a conceptual offshore wind turbine driven electricity and thermocline energy extraction plant", *Renew. Energ.*, **68**, 853-867.
- Daroczy, L., Janiga, G., Petrasch, K., Webner, M. and Thevenin, D. (2015), "Comparative analysis of turbulence models for the aerodynamic simulation of H-Darrieus rotors", *Energy*, **90**, 680-690.
- Fuglsang, P. and Madsen, H.A. (1999), "Optimization method for wind turbine rotors", *J. Wind Eng. Ind. Aerod.*, **80**, 191-206.
- Giguere, P. and Selig, M.S. (1997), "Low Reynolds Number airfoils for small horizontal axis wind turbines", *Wind Eng.*, **21**, 367-380.
- Henriques, J.C.C., Marques da Silva, F., Estanqueiro, A.I. and Gato, L.M.C. (2009), "Design of a new urban wind turbine airfoil using a pressure-load inverse method", *Renew. Energ.*, **34**, 2728-2734.
- Karhikeyan, N., Kalidas, M.K., Arun, K.S. and Rajakumar, S. (2015), "Review of aerodynamic developments on small horizontal axis wind turbine blade", *Renew. Sust. Energ. Rev.*, **42**, 801-822.
- Khamlaj, T.A. and Rumpfkeil, M.P. (2018), "Analysis and optimization of ducted wind turbines", *Energy*, **162**, 1234-1252.
- Sadikin, A., Yunus, N.A.M., Abd Hamid, S.A., Ismail, A.E., Salleh, S., Ahmad, S., Rahman, M.N.A., Mahzan, S. and Ayop, S.S. (2018), "A comparative study of turbulence models on aerodynamic characteristics of a NACA0012 airfoil", *Int. J. Integr. Eng.*, **10**, 134-137.
- Tangler, J.L., Somers, D.M. (1995), NREL Airfoil Families for HAWTS, National Renewable Energy Laboratory.
- Vardar, A. and Alibas, İ. (2008), "Research on wind turbine rotor models using NACA profiles", *Renew. Energ.*, **33**, 1721-1732.

Nomenclature

c : Chord Length
 C_d : Drag Coefficient
 C_l : Lift Coefficient

Subscripts

max : Maximum

